Particle size distributions in a region of coastal upwelling analyzed by characteristic vectors[1]

James C. Kitchen, David Menzies, Hasong Pak, and J. Ronald V. Zaneveld
School of Oceanography, Oregon State University, Corvallis 97331

Abstract

Particle size distributions (8–105-μm diameter), chlorophyll *a*, and particulate carbon were measured off the Oregon coast during July 1973. The particle counts were transformed to volume concentration and then subjected to characteristic vector analysis. Ninety-two percent of the variance was accounted for by linear combinations of the first two characteristic vectors. Two weighting factors define the proportions of the two characteristic vectors which will, when added to the mean volume concentration curve, approximate the actual data for each sample. Variations in the first weighting factor correspond well with variations in total volume. Changes in the second weighting factor indicate which segment of the size range contains the largest proportion of the particulate volume. Comparison with temperature and salinity data indicated that the near surface water with proportionately large volumes of particles less than 20 μm was warmer and less saline than the surface waters with large volumes between 20 and 50 μm. High correlation with particulate carbon and chlorophyll suggests that in both cases a large proportion of the particles is phytoplankton.

During the summer months, the prevailing north winds along the Oregon coast produce an Ekman transport in the surface water away from the coast, mixing the coastal water with the warmer, less saline Columbia River plume water (Pattullo and Denner 1965). This surface water is replaced by cold deep water upwelled near the coast. This nutrient-rich water can then support large phytoplankton blooms. The phytoplankton act as particulate tracers of the water masses and thus can be used to describe the dynamics of the circulation (Jerlov 1968; Pak et al. 1970*b*). Unfortunately, phytoplankton have their own growth dynamics, rendering any conservative assumption questionable. This fact limits the use of total particulate volume for sensitive water mass characterizations.

An alternative method describing a collection of particles is by the particle size distribution (psd)—the number of particles or the particulate volume as a function of some size parameter (often the diameter). Suspended material in the oceans and many other natural collections of particles often have a psd which is fitted very well by the hyperbolic curve $N = kx^{-c}$ (Bader 1970) where N is the number of particles larger than diameter x, and k and c are constants. Growing phytoplankton populations do not necessarily fit this curve. Carder et al. (1971) suggest the Weibul distribution [$F = 1 - \exp\ (-r/r_0)^c$ where r is the particle radius, r_0 the scale parameter, c the shape parameter, and F the relative frequency] to account for the larger number of big phytoplankton particles. Neither is adequate for near-surface water in the Oregon upwelling region. The bumps and peaks in the observed psd curves cannot be described by these exponential forms. Parsons (1969) described similar distributions by an index of diversity $D = \Sigma\ P_i \log P_i$ where P_i is the fraction of the total volume in the ith band, the range of volume in each band being twice the range of the band preceding it. This gives a single value corresponding to community diversity as measured by species counts, but the size distribution cannot be reconstructed from it. The irregularity of the psd curves presents a problem in showing them and in their correlation

[1] This investigation has been supported by Office of Naval Research contract N00014-67-A-0369-0007 under project NR 083-102 and by the Coastal Upwelling Ecosystems Analysis Program of the International Decade of Ocean Exploration through grant GX41561.

with other data. This report illustrates a method for reducing the number of parameters needed to describe the psd adequately and applies it to data obtained in an area of coastal upwelling.

Method

The data analyzed in this report was obtained during a 10-day multidisciplinary coastal upwelling experiment (CUE) cruise in late July 1973—a period of active upwelling. Discrete samples were obtained by a pumping system attached to an STD with deck readout. Sampling depths were selected to characterize the source of the upwelling water, the surface euphotic zone (where phytoplankton growth takes place), the pycnocline, and the thermal inversion when present.

Particle size distributions were measured from 8–105-μm diameter in twelve bands with a model A Coulter counter interfaced to a Nuclear Data 2400 multichannel analyzer. Phytoplankton standing stock was measured as chlorophyll *a* concentration, determined by a continuous flow Turner 111 fluorometer, and as particulate carbon, determined by combustion of glass fiber filters in a Carlo Erba model 1100 CHNO elemental analyzer.

The particle count data were reduced to the form of volume concentration in ppm normalized by dividing by the bandwidth in micrometers, so that the total volume is equal to the area under the psd curve. These numbers were subjected, with the aid of a computer, to characteristic vector analysis (CVA), the steps of which are outlined by Simonds (1963). Part of his discussion is slightly rephrased below.

Given r data points for each sample and N number of samples, the data consist of a matrix of N rows and r columns. CVA involves computing the variance-covariance matrix S from this. Characteristic vectors (CV) are obtained corresponding to the latent roots (λ) of the determinental equation $|S - \lambda I| = 0$ where I is an r by r unit matrix. This procedure produces a set of row vectors, $V_1, V_2, \ldots, V_r$, which when added in the proper amounts to the mean

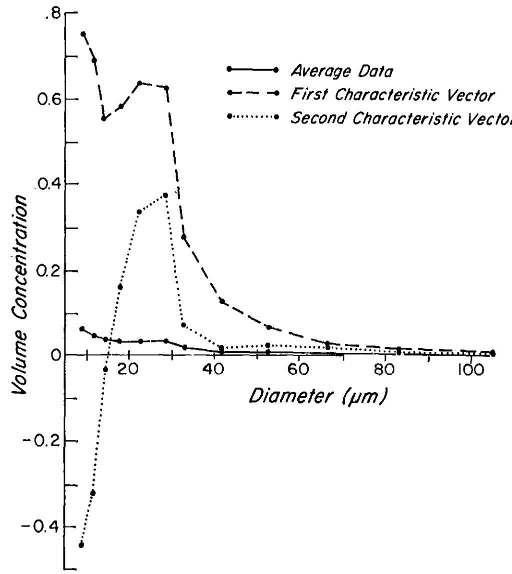

Fig. 1. The normalized volume concentration (ppm/μm bandwidth) for the average of the 263 samples, the first characteristic vector, and the second characteristic vector.

row vector of data (the mean of each of the psd bands for the whole data set) will reproduce the actual data. An advantage of this method is that most of the variability will usually be accounted for by the first few vectors, thus reducing the number of variables. These CV factors will be statistically independent but do not necessarily have physical significance (Simonds 1963). CVA has been used by Mueller (1973) in studying ocean color spectra and by Kopelevich and Burenkov (1972) for light scattering functions.

Results

For the 263 samples analyzed in this study, the CVA method indicates that the first CV removes 74% of the variance, the second CV removes 18%, and the third CV only 3%. Thus, for a given sample:

$$C_1 \cong \langle C_1 \rangle + W1V_{1,1} + W2V_{2,1}$$
$$C_2 \cong \langle C_2 \rangle + W1V_{1,2} + W2V_{2,2}$$
$$\vdots$$
$$C_{12} \cong \langle C_{12} \rangle + W1V_{1,12} + W2V_{2,12};$$

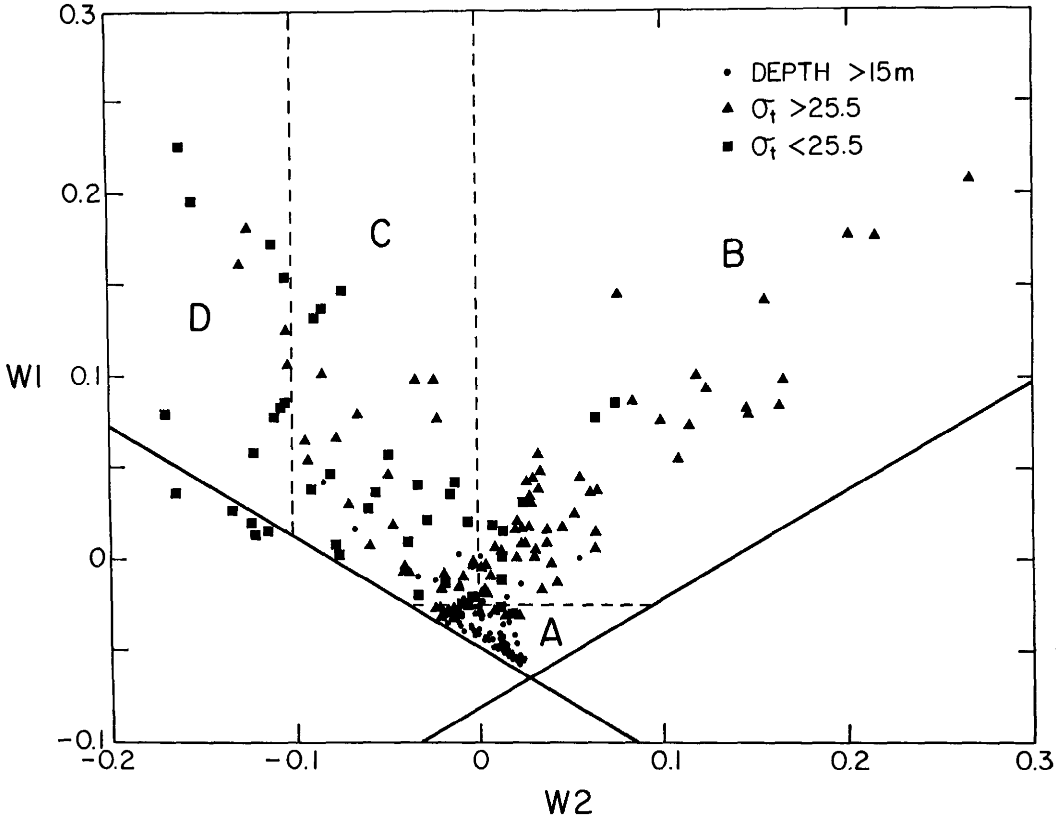

Fig. 2. The distribution of the first characteristic vector weighting factors ($W1$) versus the second characteristic vector weighting factors ($W2$). Points in region A represent primarily samples taken below the ephotic zone. The other groups are predominantly samples from the top 15 m. Samples from the surface layer are coded according to their sigma-t values.

C_i is the volume concentration for the sample in the ith psd band, $\langle C_i \rangle$ is the average concentration in the ith band for all the samples, $W1$ and $W2$ are the weighting factors determined for the sample, and $V_{1,i}$ and $V_{2,i}$ are the ith components of the first and second CV determined for the entire sample set. The average vector and the two CV curves are shown in Fig. 1. CVA has reduced the 12 psd values to two parameters with little loss of information.

The first CV weighting factors ($W1$) have been plotted against the second CV weighting factors ($W2$) in Fig. 2 for all samples analyzed. Samples from the homogeneous, clean, deep water are shown as a dense patch of points with $W1$ values near –0.05. Samples from the surface waters form the two arms, one with positive $W2$ values and one with negative $W2$. Notice that the positive arm represents almost exclusively samples with sigma-t greater than 25.5. To see what these arms mean, the sum of the average data and different proportions of the two CV curves has been plotted in Fig. 3. The total volume varies most with $W1$. Negative $W2$ values indicate that a large fraction of the particulate volume is contributed by particles with diameters less than 20 μm, and positive $W2$ values represent samples that have a well defined peak in volume concentration between 20- and 50-μm diameter.

The slanted lines on Fig. 2 indicate the region of possibility. That is, below these

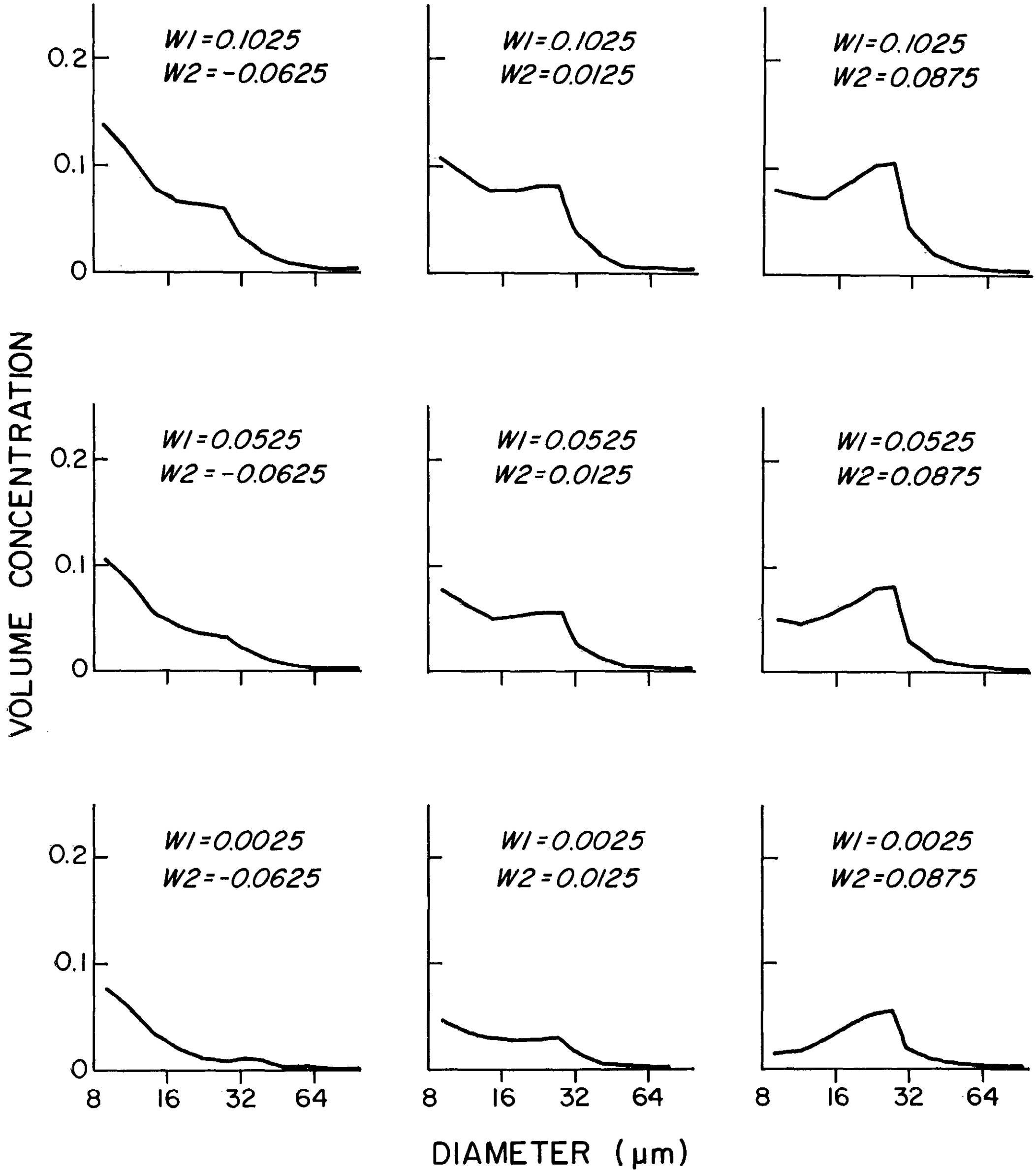

Fig. 3. The sum (ppm/μm bandwidth) of the average volume concentration curve and various proportions of the two characteristic vectors as defined by their weighting factors, $W1$, $W2$.

lines the sum of the average vector and the weighted characteristic vectors produces negative volume concentrations in certain psd bands; i.e. below the line with negative slope

$$\langle C_6 \rangle + W1V_{1,6} + W2V_{2,6} < 0,$$

and below the line of positive slope

$$\langle C_1 \rangle + W1V_{1,1} + W2V_{2,1} < 0.$$

These particular bands are the first to go negative in each case. Since negative volume has no meaning here, these lines delineate the region of possibility. The reason

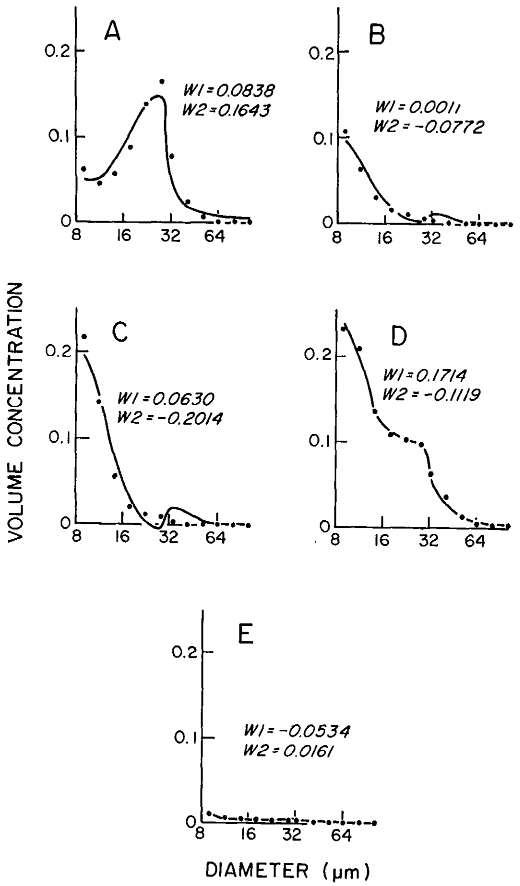

Fig. 4. Volume concentration (ppm/μm bandwidth) as given by the measured data (dots) and by the characteristic vector representations (lines) for samples taken d km from shore at a depth z, (d,z) as follows: A—(1.85,1); B—(37,1); C—(15,5); D—(9.25,1); E—(7.5,20).

that some points do, in fact, lie outside this region is that not all of the variation is accounted for by the first two characteristic vectors. The psd curves of the actual data represented by points outside the region of possibility have high volume concentration at the lowest diameter measured and fall rapidly with increasing size. The psd values represented by points almost on but above the line are very smooth in shape, and those farther removed are more irregular. The other lines and letters in Fig. 2 are used in later discussions. In Fig. 4 the volume concentration curves for some representative samples are given along with their CV representation. The samples were chosen to illustrate the variations discussed above.

To illustrate the use of the two CV weighting factors, we shall compare two transects. The first is along a line of 45° 05′N lat off the Oregon coast. Figure 5a shows the resulting distribution of the first CV weighting factors $W1$. A large mass of deep water tends toward the surface near the coast. This water mass is low in particulate matter since the negative values of $W1$ indicate a subtraction from the mean volume concentration curve. At sta. 2, large values of $W1$ indicate a large concentration of particles, corresponding well with the distribution of chlorophyll a (Fig. 5b) and of particulate carbon (Fig. 5c). Notice, in all three diagrams, that the water with the lowest values of each parameter is nearest the surface at sta. 4. Chlorophyll a concentration is as intense at sta. 6 as at sta. 2, and yet the $W1$ values are not nearly as great as at 2. Total particulate volume (Fig. 5d) shows the same pattern as $W1$. If we look at the distribution of the second CV weighting factors $W2$ (Fig. 5e) we find negative values at sta. 6 and positive values at sta. 2. Recalling the discussion of Fig. 3, this means that a greater proportion of the particulate volume is accounted for by smaller particles at sta. 6 and that a greater proportion of the volume at sta. 2 represents particles between 20 and 50 μm. If we now look at the temperature distribution (Fig. 5f), we see that the two stations are separated by a large temperature gradient, the inshore station being much colder.

Figure 6 shows $W1$, $W2$, and temperature for a transect taken a day later at 45° 12.2′N lat. A significant temperature inversion is noticeable at three consecutive stations, and the large temperature gradient seen in the previous transect is not present. Low surface temperatures are prevalent throughout the transect. Correspondingly, all samples from the surface layer have large positive values of both $W1$ and $W2$ increasing with distance from shore. Thus,

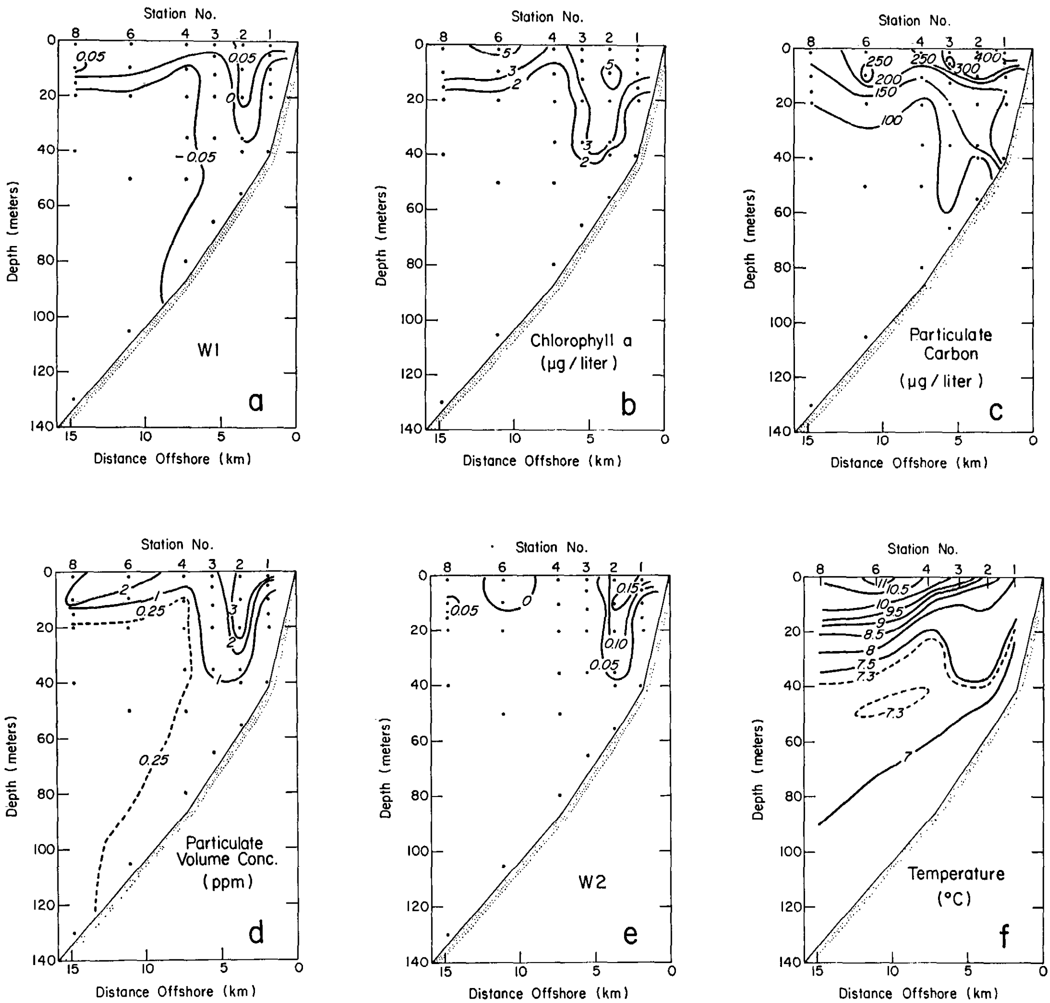

Fig. 5. A transect sampled 30 July 1973 along 45°05′N lat off the Oregon coast. (Temperature distribution was measured continuously by an STD.)

we have seen two different distributions of psd which seem to be related to the temperature structure.

To compare the *W*1–*W*2 water mass characterization with the standard temperature-salinity diagrams, we constructed Fig. 7. It is a *T–S* diagram with the points coded according to their position on the *W*1–*W*2 diagram. Each kind of symbol represents one of the regions marked off in Fig. 2. The boundaries of these regions are our rough visual estimate of the separation of the features of Fig. 2. On Fig. 7 the symbols form overlapping but distinct groups of points. In general, the diagram shows that warmer, less saline water contains a greater proportion of small particles (as evidenced by negative *W*2 values) than the cold, salty water. The points representing samples with *W*1 values less than –0.025 (group A) have a broad range of temperature and salinity but for a given salinity are usually colder than the other three groups. Group A, therefore, represents predominately deep samples, and, as mentioned before, the negative *W*1 component indicates a subtraction from the mean volume concentration curve and,

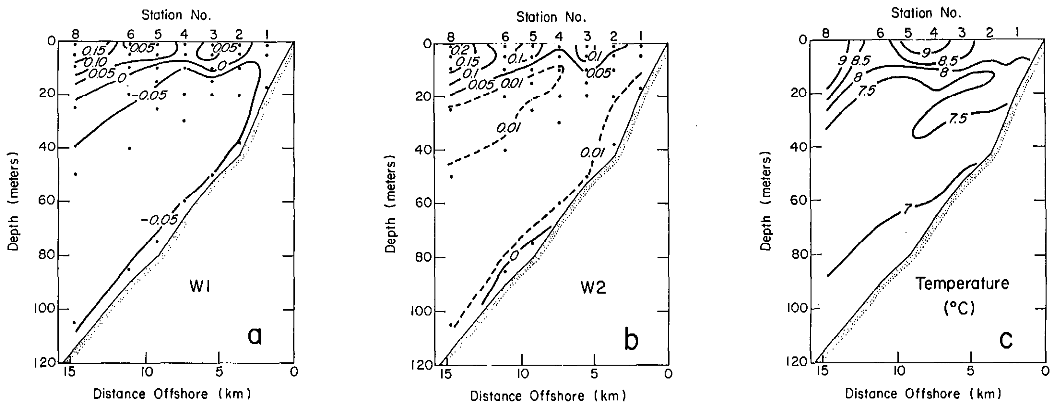

Fig. 6. A transect sampled 31 July 1973 along 45°12.2′N lat off the Oregon coast. (Temperature distribution was measured continuously by an STD.)

therefore, water with less particulate matter. Group B is concentrated below 10°C and groups C and D are spread through the warmer, less saline water. The averages of temperature and salinity (T, S) for the groups are: A—(7.61, 33.47); B—(8.31, 33.41); C—(9.35, 33.01); D—(10.49, 32.65). The data for the station producing the outlying group of points at the top of Fig. 7 have not been used in these averages. This group of points represents a station taken 75 km from shore, the farthest out we went and is believed to be an isolated station in an open ocean water mass.

Discussion

Parsons (1969) presented psd curves very similar to those presented here. In his study, change in particulate volume compared favorably with production as determined by the ^{14}C method. Also, the correlation of particulate volumes with carbon and chlorophyll *a* was highly significant. In our study, the weighting factors W1 and

Table 1. Regression comparison of particulate volume and CV weighting factors vs. chlorophyll a *and particulate carbon.*

Regression equation	R	df	levels of sign
CHL = 0.99(±0.12) + 1.35(±0.07)VOL*	0.78	260	< 0.001
CHL = 2.65(±0.07) + 31.5(±1.2)W1	0.86	260	< 0.001
CHL = 0.60(±0.1) + 5.12(±0.28)V_{1-3} + 0.49(±0.14)V_{4-6} †	0.87	260	< 0.001
CHL = 2.65(±0.07) + 31.5(±1.2)W1 - 7.3(±1.1)W2	0.88	260	< 0.001
CARB = 89.97(±9.4) + 68.9(±5.3)VOL	0.64	249	< 0.001
CARB = 175.0(±6.2) + 1658.9(±101.7)W1	0.72	249	< 0.001
CARB = 68.65(±9.0) + 243.95(25.3)V_{1-3} + 41.61(±12.3)V_{4-6}	0.726	249	< 0.001
CARB = 175.0(±6.1) + 1667.3(±100.4)W1 - 271.4(±98.6)W2	0.730	249	< 0.001

* Numbers in parentheses are the standard errors of the regression coefficients.

† V_{1-3} is the particulate volume in the first three particle size distribution bands, and V_{4-6} is the volume in bands 4 through 6 of the particle size distributions.

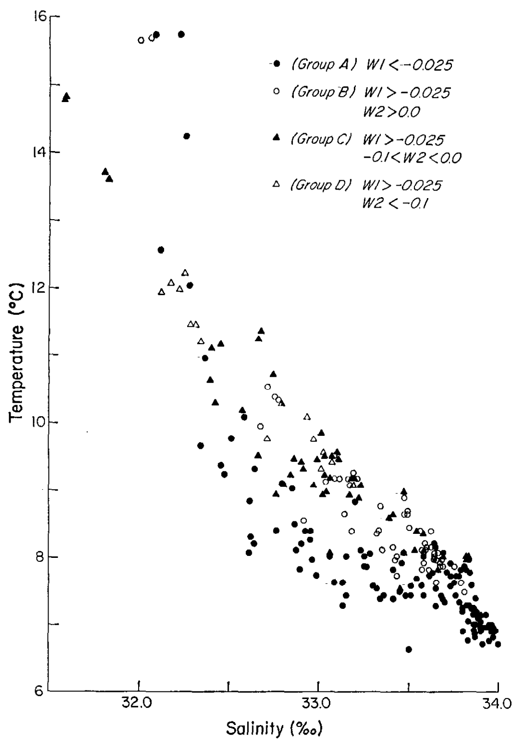

Fig. 7. A temperature–salinity plot of the samples coded according to their characteristic vector weighting factors. Each type of symbol represents one of the regions outlined in Fig. 2.

*W*2 also correlate well (Table 1) with particulate carbon and chlorophyll *a*, leading us to conclude, as did Parsons, that the large particulate volumes are composed primarily of living phytoplankton. Accepting Parsons' designated value of 20-μm diameter as the boundary between nanoplankton and microplankton, negative *W*2 values indicate a predominance of nanoplankton and positive *W*2 values that most of the particulate volume represents the larger microplankton.

Table 1 shows that, for our 263 samples, *W*1 correlates better with carbon and chlorophyll *a* than does total measured volume. Also, a linear combination of *W*1 and *W*2 correlates with chlorophyll *a* and carbon equally well as a linear combination of the volume in the first three psd bands (*V*1–3) and the volume in the second three bands (*V*4–6). Thus, for some applications at least, we lose nothing by using CV weighting factors instead of volume. In fact, we gain psd shape information that volumes alone do not give us. Recalling the discussion of Fig. 2 and the illustrations of Fig. 4, a lot of qualitative information is given by the weighting factors that cannot be expressed in terms of ratios of volumes.

The features of Fig. 2 itself are interesting. Foremost is the lack of points in the top center. This suggests that size distributions similar to the first CV (e.g. the case that $W2 \cong 0.0$ and $W1 > 0.1$) are lacking. Figure 1 shows that the first CV has large volumes of both microplankton and nanoplankton. The lack of similar curves in the data suggests that competition from the microplankton keeps the nanoplankton from reaching proportionately large numbers in the nutrient-rich upwelled water. Of course, our measurements cover only the largest members of the nanoplankton, but an interaction is definitely indicated.

A second interesting feature is the cluster of points at the bottom of Fig. 2. The dense patch of points there forms a line parallel to the left boundary of the region of possibility discussed earlier. Recalling from that discussion that points near this boundary represented psd curves that tended to have a very smooth shape and considering that these are deep samples that would have a lesser proportion of living organisms, we would expect these points to have smooth distributions also. In fact, for samples with *W*1 less than –0.04, 83% of the correlation coefficients for the fit to the hyperbolic psd are greater than 0.99 and the best coefficient is 0.9996. For all other samples, only 44% have correlation coefficients greater than 0.99.

Except for a few samples, the positive *W*2 leg represents water with sigma-*t* values greater than 25.5. The negative *W*2 leg has two extensions. The extension along the lower boundary is comprised of samples having lower density ($\sigma_t < 25.5$). The rest of this leg seems to be equally represented by both water types. The samples with CV weighting factors not near the lower boundary have psd curves similar to

D of Fig. 4. Even though the smaller particles predominate, there is still a large population of microplankton. Many of these samples have sigma-*t* values near 25.5. This suggests that, as the upwelled water moves offshore, the microplankton stock first increases (as evidenced in Fig. 6), then is mixed with the smaller particles of the Columbia River plume. As the effect of the Columbia River plume becomes greater, the microplankton become less significant. This can be seen more clearly in Fig. 7. The group B samples, representing the positive leg of Fig. 2, are densely packed around a salinity of 33.6‰, thinned out in fresher water, and eliminated in water less saline than 32.5‰ except for the open ocean station mentioned previously.

The discussion of Fig. 7 pointed out a temperature-salinity relationship of the CV weighting factors. This relationship is probably not due primarily to a temperature or salinity dependence, but to the abundance of nutrients. Two distinct water masses are common in this nearshore region at this time of year—the upwelled water and the Columbia River plume water (Pak et al. 1970*a*). The Columbia River plume water is characterized by lower salinity, higher temperature, and depleted nutrients. The difference in the temperature structure between the two transects is then related to differences in the interaction of the two water masses. Thus the $W1$–$W2$ distribution is determined by and characterizes the circulation. The large difference between the two groups of points representing these water masses (Fig. 2) indicates that the weighting factors provide a sensitive characterization of water mass.

Conclusion

Characteristic vector analysis has been shown to describe the particle size distributions very well, and qualitative changes in the psd bands have, in turn, been shown to give information about the biology and dynamics of a region. As more and better data become available, the biological community structure can be studied more thoroughly and the method extended to study other problems of the upwelling region. The origin of the particles associated with the temperature inversions and the changes in the psd curves that denote the inception and demise of an upwelling event are problems that come immediately to mind. Particle size distributions are useful descriptive factors for correlating biological processes, circulation, and optical measurements. Characteristic vector analysis has been shown to provide a method of reducing psd curves to a few parameters that can be more easily handled statistically and conceptually and can be graphically presented so as to indicate qualitative as well as quantitative changes.

References

BADER, H. 1970. The hyperbolic distribution of particle sizes. J. Geophys. Res. **75:** 2823–2830.

CARDER, K. L., G. F. BEARDSLEY, JR., AND H. PAK. 1971. Particle size distributions in the eastern equatorial Pacific. J. Geophys. Res. **76:** 5070–5077.

JERLOV, N. G. 1968. Optical oceanography. Elsevier.

KOPELEVICH, O. V., AND V. I. BURENKOV. 1972. Statistical characteristics of the light scattering functions of sea water, p. 126–136. *In* Optics of the ocean and the atmosphere. Nauka, Leningrad.

MUELLER, J. L. 1973. The influence of phytoplankton on ocean color spectra. Ph.D. thesis, Oregon State Univ., Corvallis. 239 p.

PAK, H., G. F. BEARDSLEY, JR., AND P. K. PARK. 1970*a*. The Columbia River as a source of marine light-scattering particles. J. Geophys. Res. **75:** 4570–4578.

———, ———, AND R. L. SMITH. 1970*b*. An optical and hydrographic study of a temperature inversion off Oregon during upwelling. J. Geophys. Res. **75:** 629–636.

PARSONS, T. R. 1969. The use of particle size spectra in determining the structure of a plankton community. J. Oceanogr. Soc. Jap. **25:** 6–15.

PATTULLO, J., AND W. DENNER. 1965. Processes affecting seawater characteristics along the Oregon coast. Limnol. Oceanogr. **10:** 443–450.

SIMONDS, J. L. 1963. Application of characteristic vector analysis to photographic and optical response data. J. Opt. Soc. Am. **53:** 968–974.

Submitted: 10 February 1975
Accepted: 14 April 1975